Overturning of Retrofitted Rocking Structures under Pulse-Type Excitations

Elias G. Dimitrakopoulos[1] and Matthew J. DeJong, M.ASCE[2]

Abstract: Numerous existing structures exhibit rocking behavior during earthquakes, and there is a continuing need to retrofit these structures to prevent collapse. In addition, while rocking behavior is typically prevented instead of utilized, an increasing number of structures are being designed or retrofitted to allow rocking motion as a means of seismic isolation. This paper investigates the use of viscous damping to limit the rocking motion by characterizing the fundamental behavior of damped rocking structures through analytical modeling. A single rocking block analytical model is used to determine the viscous damping characteristics, which exploit the beneficial aspects of the rocking motion, while dissipating energy and preventing overturning collapse. To clarify the benefits of damping, overturning envelopes for pulse-type ground accelerations are presented and compared with the pertinent envelopes of the free rocking block. A semianalytical solution to the linearized equations of motion enables rapid generation of collapse diagrams for pulse excitations, which provide insight into the overturning mechanisms of the damped rocking block and the sensitivity of the response to the parameters involved. In addition, through solution of the nonlinear equations of motion, bilateral and unilateral linear viscous dampers are shown to provide similar benefit toward preventing overturning, while nonlinear damping is found to provide relatively little and inconsistent benefit with respect to linear damping. **DOI: 10.1061/(ASCE)EM.1943-7889.0000410.** © *2012 American Society of Civil Engineers.*

CE Database subject headings: Rock structures; Excitation; Rehabilitation; Earthquakes.

Author keywords: Rocking; Overturning; Analytical dynamics; Earthquake engineering; Damping.

Introduction

Numerous structures experience rocking when loaded dynamically, including monuments, towers, bridge piers, and sculptures. Recent earthquakes have increased worldwide incentive to retrofit such structures to avoid collapse during dynamic loading. In addition, structures are increasingly being designed to capitalize on the beneficial seismic isolation effect of allowing rocking motion, but optimal design configurations are still needed.

Typically, rocking behavior is prevented instead of limited or controlled. Prevention is achieved by tying structures down, which may involve internal drilling and reinforcing, or external wrapping with fiber-reinforced polymers (Pampanin 2006). Recently though, the exploitation of rocking behavior, supplemented with additional strength and/or damping, is proliferating. The most important asset of the rocking isolation is the avoidance of loading on the structure, which limits yielding and damage. However, rocking does have the palpable drawback of higher overturning risk.

Rocking has been proposed as a seismic isolation technique for bridges (Chen et al. 2006). More recently, the rocking behavior of bridge piers on footing foundations has been studied analytically and/or experimentally by Ugalde et al. (2010), Cheng (2007), and Hung et al. (2011). The combined use of rocking and additional strengthening and/or damping has also been investigated. Marriott et al. (2009) proposed the use of rocking-dissipating connections for bridge piers, Pollino and Bruneau (2007) made similar suggestions for steel truss piers, and ElGawady and Sha'lan (2011) investigated the seismic behavior of segmental bridge bents. For buildings, similar approaches are proposed by Restrepo and Rahman (2007) for wall elements, Roh and Reinhorn (2010) for columns, Ajrab et al. (2004) for wall-frame structures, and Rai and Goel (2007) for masonry buildings.

Notwithstanding the applicable value of many studies on rocking systems available in the literature, this research redirects attention to the fundamental dynamics governing the response of rocking systems supplemented with additional strength or damping. In contrast to the significant amount of basic analytical-theoretical research on the response of stand-alone rocking structures (see Augusti and Sinopoli (1992) and references therein), there are relatively few theoretical studies on the response of retrofitted rocking structures. For instance, the seismic isolation of rocking objects was considered by Caliò and Marletta (2003), Contento and Di Egidio (2009; Di Egidio and Contento 2009), or more recently by Vassiliou and Makris (2012). Makris and Zhang (2001) analyzed the behavior of the anchored block under pulse-type ground motions and showed that the anchored rocking response can be worse than that of the pertinent stand-alone rocking block.

Complementing the research of Makris and Zhang (2001), the next section shows that the use of a central tendon can overstiffen the rocking block, store energy in the system, and be destructive. Furthermore, when earthquake loading is rare and relatively minimal, as in the U.K., extensive reinforcing of a vast number of structures may be economically infeasible and too invasive for heritage structures. Hence, application of intelligent less invasive intervention methods is sought, through limitation of the rocking response instead of prevention. This motivates the use of damping as a retrofit technique. This research aims to fundamentally characterize the

[1]Assistant Professor, Dept. of Civil and Environmental Engineering, The Hong Kong Univ. of Science and Technology, Clear Water Bay, Kowloon, Hong Kong (corresponding author). E-mail: ilias@ust.hk

[2]Lecturer, Dept. of Engineering, Univ. of Cambridge, Trumpington St., Cambridge CB2 1 PZ, U.K. E-mail: mjd97@cam.ac.uk

Note. This manuscript was submitted on May 23, 2011; approved on February 9, 2012; published online on February 11, 2012. Discussion period open until January 1, 2013; separate discussions must be submitted for individual papers. This paper is part of the ***Journal of Engineering Mechanics***, Vol. 138, No. 8, August 1, 2012. ©ASCE, ISSN 0733-9399/2012/8-963–972/$25.00.

damped rocking response to pulse-type ground motions, in order to lay the foundation for the development of new retrofit solutions. Pulse-type motions are used as the primary pulses within near-source ground motions and have been shown to govern the rocking response (Zhang and Makris 2001; DeJong et al. 2008).

Anchored Rocking Motion

Before considering damping retrofit solutions, consider first the rocking block retrofitted with an unbonded central tendon (Fig. 1). This simple configuration is representative of retrofit solutions used in practice, but its dynamic response has received relatively little attention in academic literature. Assuming the coefficient of friction is high enough to prevent sliding during base excitation, the rocking motion initiates when the ground acceleration $\ddot{u}_g$ exceeds the critical value: $\ddot{u}_g \geq a_{g,}\min = g\tan(\alpha)$, where α is the angle of slenderness and g is the acceleration of gravity. During the rocking motion, moment equilibrium with respect to the pivot points (O or O′) gives

$$I_0\ddot{\theta} + mgR\sin[\alpha\,\mathrm{sgn}(\theta) - \theta] + Kb^2\sin\theta = -m\ddot{u}_g R\cos[\alpha\,\mathrm{sgn}(\theta) - \theta] \quad (1)$$

where θ = rocking rotation (positive in the clockwise direction), I_0 = moment of inertia with respect to the pivot point, m = mass of the block, R = length of the half-diagonal, K = stiffness, T = force of the tendon, and sgn() = the standard sign function. The slenderness angle is defined by $\tan(\alpha) = b/h$, where $2b$ is the width and $2h$ is the height of the block. The tendon is assumed to behave elastically until brittle fracture occurs at an elongation of u_f. The yield elongation u_f of the tendon occurs, assuming small rotations, at a rotation $\theta_f : u_f \simeq b\theta_f$.

After dividing by I_0, the equation of motion [Eq. (1)] can be written in the compact form

$$\ddot{\theta} = \begin{cases} -p^2[\sin[a\,\mathrm{sgn}(\theta) - \theta] + \frac{\ddot{u}_g}{g}\cos[a\,\mathrm{sgn}(\theta) - \theta] + \frac{3}{4}\frac{\alpha}{q}\sin\alpha^2\sin\theta], & \text{if } t < t_f \\ -p^2[\sin(\alpha\,\mathrm{sgn}(\theta) - \theta) + \frac{\ddot{u}_g}{g}\cos(\alpha\,\mathrm{sgn}(\theta) - \theta)], & \text{if } t > t_f \end{cases} \quad (2)$$

where $p = \sqrt{mgR/I_0}$ is the frequency parameter of the block, which is equal to the small angle pendulum frequency of the block when hung from its corner; for a rectangular block $I_0 = 4mR^2/3$, which yields $p = \sqrt{3g/4R}$. Further, following (Makris and Zhang 2001), $q = u_f p^2/g$ is the influence factor, $\sigma = F_u/W$ is the strength parameter, F_u is the strength of the tendon, and W is the weight of the block. If the tendon reaches the fracture elongation $\theta(t) = u_f/b = \theta_f$, say at time instant t_f, the tendon snaps and the equation of motion switches irreversibly to the lower part of Eq. (2).

To complete the description of the problem, the equation of motion is complemented with a coefficient of restitution η, which defines the energy dissipated when the block impacts the base (and switches pivot points) as the ratio of the pre- and postimpact velocities

$$\dot{\theta}^+ = \eta\dot{\theta}^- \quad (3)$$

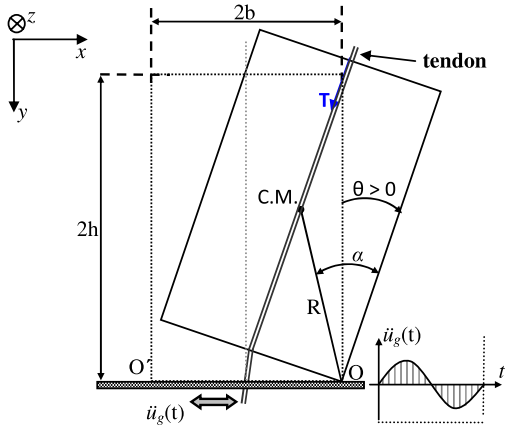

Fig. 1. Rocking block retrofitted with a central tendon

This approach is reasonable under the assumption that after each base impact, the block remains in contact with the new impact point. In other words, the block is slender enough to prevent bouncing or sliding (Contento and Di Egidio 2009).

Eqs. (2) and (3) can now be used to determine the rocking response of the retrofitted block. Comparison of Eq. (2) with the pertinent formulation for the rocking block retrofitted with anchors located at both bottom corners (Makris and Zhang 2001) reveals that, for small rotations, the central tendons must be four times stiffer and twice as strong as the corner anchors to create an equivalent system.

The effect of adding a central tendon to the overturning envelope of the rocking block subjected to a single sinusoidal ground acceleration pulse is shown in Fig. 2. The overturning plot (Fig. 2) is typical of rocking systems, and predicts overturning after impact for ground acceleration pulses that lie within the lower bubble, overturning without impact in the upper left region, and no overturning for all other pulses. Fig. 2 demonstrates that for low-frequency acceleration pulses, the minimum acceleration needed to overturn the block is increased by the tendon, while for higher-frequency pulses the tendon provides little benefit or can even be destructive. While increasing the strength of the tendon increases the minimum acceleration needed to overturn the block, it also increases the tendency of the block to overturn after impact (Fig. 2). This counterintuitive trend, previously observed for corner anchored blocks (Makris and Zhang 2001), results from the stiff tendon attracting load and storing energy in the system. In particular, the energy stored in the tendon during the initial cycle of rocking propels the block at a higher angular velocity in the other direction after impact, and eventually causes the tendon to snap and the block to collapse at lower acceleration levels. The response is even worse for elastoplastic anchored blocks (Makris and Zhang 2001). Furthermore, the stresses within the structure are significantly increased by the presence of the tendon.

J. Eng. Mech. 2012.138:963-972.

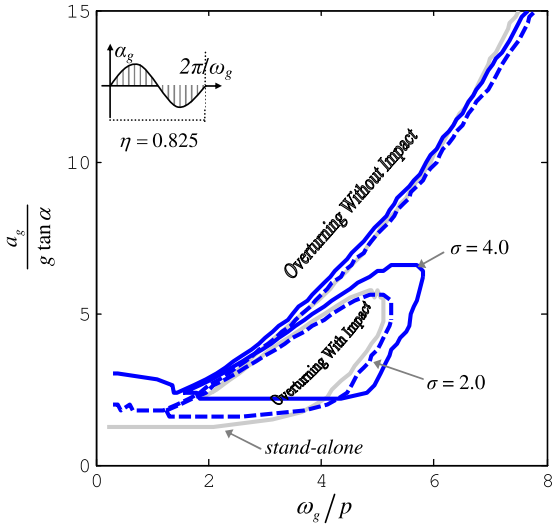

Fig. 2. Overturning envelopes for the freestanding block and the block retrofitted with a central tendon with strength parameters $\sigma = 2.0$, 4.0 and $q = 5.2 \times 10^{-4}$

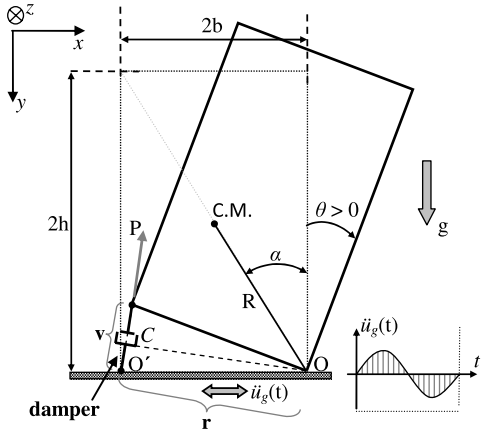

Fig. 3. Rocking block retrofitted with viscous dampers at its corners

Damped Rocking Motion: Semi-Analytical Approach

Motivated by the inverse effects of adding strength to the rocking block, and the beneficial seismic isolation effect of allowing the rocking motion, the remainder of the this paper focuses on the effects of additional damping instead of additional strength.

This section presents a semianalytical approach to predicting the damped rocking response, which is based on linearized equations of motion. The linearization presented was shown to sacrifice relatively little accuracy for slender blocks (Lenci and Rega 2006), and the semianalytical approach is considerably less computationally expensive than the numerically solved nonlinear approach, particularly when producing multiple overturning envelopes. Thus, the semianalytical approach allows rapid assessment of the trends caused by varying the range of system parameters. The numerical nonlinear solution will be used in the subsequent section to investigate nonlinear damping in detail.

Consider the rocking block retrofitted with linear viscous dampers at its corners and subjected to a pulse-type base excitation with acceleration amplitude a_g and frequency ω_g. Under the assumptions in the previous section (no sliding and bouncing), the moment equilibrium of the retrofitted rocking block with respect to pivot points O and O′ (Fig. 3) gives

$$I_0 \ddot{\theta} + mgR \sin[\alpha \operatorname{sgn}(\theta) - \theta] + P \cdot r = -m\ddot{u}_g R \cos[\alpha \operatorname{sgn}(\theta) - \theta] \tag{4}$$

where r = lever arm of the damping force P with $P = C\dot{v}$, $\dot{v}$ = extension velocity of the damper, and C = damping constant. Eq. (4) can be rewritten using geometric properties

$$\ddot{\theta} = -p^2 \left\{ \sin[\alpha \operatorname{sgn}(\theta) - \theta] + \frac{\ddot{u}_g}{g} \cos[\alpha \operatorname{sgn}(\theta) - \theta] \right\} - p\gamma(1 + \cos\theta)\dot{\theta} \tag{5}$$

where $p = \sqrt{3g/4R}$ is again the frequency parameter of the block, and $\gamma = (3C\sin^2\alpha)/(2mp)$ is a dimensionless parameter that relates the damping constant C to the mass m, slenderness α, and frequency p of the block. When the block is slender enough (small α) that the rotation θ remains small, and assuming a simple trigonometric excitation of the form

$$\ddot{u}_g = \begin{cases} a_g \sin(\omega_g t + \psi), & \text{for } t \le T_{ex} \\ 0, & \text{for } t > T_{ex} \end{cases} \tag{6}$$

Eq. (5) can be linearized as

$$\ddot{\theta} + 2p\gamma\dot{\theta} - p^2\theta + p^2\alpha \operatorname{sgn}(\theta) = \begin{cases} -p^2 \frac{a_g}{g} \sin(\omega_g t + \psi), & \text{for } t \le T_{ex} \\ 0, & \text{for } t > T_{ex} \end{cases} \tag{7}$$

where $\psi = \sin^{-1}(\alpha g / a_g)$ is the phase angle at the time instant rocking initiates and $T_{ex} = (2\pi - \psi)/\omega_g$ is the time instant when the excitation expires and the free rocking initiates. The solution for the forced rocking $t \le T_{ex}$ and the free rocking stage $t > T_{ex}$ are thus

$$\begin{cases} \theta(t) = \alpha \operatorname{sgn}(\theta) + Ae^{\lambda t} + Be^{\mu t} + \frac{p^2}{l}\frac{a_g}{g} \sin(\omega_g t + \psi + \phi), & \text{for } t \le T_{ex} \\ \theta(t - T_{ex}) = \alpha \operatorname{sgn}(\theta) + Ae^{\lambda(t - T_{ex})} + Be^{\mu(t - T_{ex})}, & \text{for } t > T_{ex} \end{cases}$$
$$\begin{cases} \dot{\theta}(t) = \lambda Ae^{\lambda t} + \mu Be^{\mu t} + \frac{p^2 a_g \omega}{gl} \cos(\omega_g t + \psi + \phi), & \text{for } t \le T_{ex} \\ \dot{\theta}(t - T_{ex}) = \lambda Ae^{\lambda(t - T_{ex})} + \mu Be^{\mu(t - T_{ex})}, & \text{for } t > T_{ex} \end{cases} \tag{8}$$

where

$$\lambda = -p\left(\sqrt{\gamma^2 + 1} + \gamma\right) < 0 \quad \cos\phi = \frac{\omega_g^2 + p^2}{l}, \quad \sin\phi = \frac{2p\gamma\omega_g}{l}$$
$$\mu = +p\left(\sqrt{\gamma^2 + 1} - \gamma\right) > 0 \quad l^2 = (\omega_g^2 + p^2)^2 + 4p^2\gamma^2\omega_g^2 \tag{9}$$

J. Eng. Mech. 2012.138:963-972.

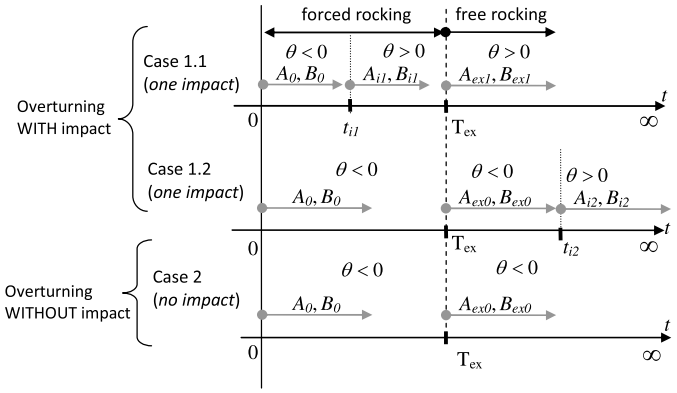

Fig. 4. Possible response sequences of a damped rocking block excited by a sine pulse. Initial conditions (A, B) and sign of rocking rotation θ for each response stage (appendix)

Eq. (8) is solved repeatedly for each subsequent stage of the rocking response. Eq. (8) is linear only during each stage of the response (Fig. 4), while because of the transition between stages the system is still nonlinear. After each impact the angular velocity of the block is reduced according to Eq. (3). The stages are separated by either impact at time t_i or the expiration of the excitation at time T_{ex}. The constants A and B depend on the initial conditions and the time instant that each stage initiates (Fig. 4). To distinguish each case, different subscripts are used. For instance, A_0 and B_0 correspond to zero initial conditions $\theta(t=0)=\theta_0$, $\dot{\theta}(t=0)=\dot{\theta}_0$. All of the quantities used are summarized in the appendix. Further, for $\gamma=0$, Eq. (8) yields the solutions of the undamped case (Zhang and Makris 2001), and for $p=1$, Eq. (8) yields the pertinent solutions of the damped rocking block for sine excitation (Lenci and Rega 2006).

The conditions that lead to overturning of the rocking block have been studied, among others, by Zhang and Makris (2001) and Makris and Roussos (1998) for the undamped case under simple trigonometric pulses, and from a dynamical systems perspective by Lenci and Rega (2006) for harmonic excitation. In this study, we extend the kinematical approach of Zhang and Makris (2001) to the damped case, according to which the minimum acceleration amplitude leads to the overturning of the block during the free rocking stage when the velocity tends to a minimum at a very large time

$$\ddot{\theta}(t_\infty)=0 \Rightarrow \lambda^2 A e^{\lambda t}+\mu^2 B e^{\mu t}=0 \Rightarrow A e^{-2\sqrt{\gamma^2+1}pt}=-\frac{\mu^2}{\lambda^2}B \tag{10}$$

As the dimensionless time pt increases, the left-hand side of Eq. (10) vanishes. Hence, for $t\to\infty$ the overturning condition [Eq. (10)] becomes

$$B=0 \tag{11}$$

Eq. (10) is the overturning condition for additional damping and unveils that under minimum acceleration amplitude, the block overturns during the free rocking phase if the coefficient B of the exponential term $Be^{\mu t}$ eventually (for large pt) disappears ($B=0$). Otherwise, because $\mu>0$ for $B>0$, the term $Be^{\mu t}$ represents exponential growth and the solution diverges [Eq. (8)]. Taking into account the different notation, the proposed overturning condition [Eq. (10)] coincides with the pertinent condition of Makris and Roussos (1998) for zero damping $\gamma=0$, while it is similar to the critical condition for immediate overturning of Lenci and Rega (2006). With the help of the appendix, the overturning condition for each case of Fig. 4 can be summarized as

$$\begin{aligned}
&\text{Case 1.1: } \ddot{\theta}(t_\infty)=0 \Rightarrow \dot{\theta}_{ex}+\lambda\alpha-\lambda\theta_{ex}=0\\
&\text{Case 1.2: } \ddot{\theta}(t_\infty)=0 \Rightarrow \eta(\lambda A_{ex0}e^{\lambda(t_{i2}-T_{ex})}\\
&\qquad +\mu B_{ex0}e^{\mu(t_{i2}-T_{ex})})+\lambda\alpha=0 \qquad (12)\\
&\text{Case 2: } \ddot{\theta}(t_\infty)=0 \Rightarrow B_0 e^{\mu T_{ex}}\\
&\qquad +(\mu-\lambda)^{-1}\frac{p^2 a_g}{gl}(\omega_g\cos\phi-\lambda\sin\phi)=0
\end{aligned}$$

The unknown time instants of impacts are determined from transcendental equations (see appendix). The numerical solution of the analytical expressions of the overturning conditions [Eq. (12)] comprise a semianalytical approach to calculate the overturning of the rocking block.

Fig. 5 presents the overturning envelopes of the rocking block with linear viscous dampers for different combinations of the coefficient of restitution η, which represents the natural damping of the system, and the additional damping γ offered by the dampers. The behavior is dependent on the following dimensionless terms:

$$\frac{a_g}{g\tan\alpha}, \qquad \frac{\omega_g}{p}, \qquad \eta, \qquad \gamma \tag{13}$$

Presenting results using the dimensionless terms in Eq. (13) allows the visualization of general trends in the rocking response, which are not limited to a single scale or geometry. Fig. 5 offers an overview of the effect of damping on the rocking block. Similar to the stand-alone rocking block (Zhang and Makris 2001), the damped rocking block displays two different modes of overturning because of a sine pulse excitation: either without impact (Case 2 in Fig. 4) or after experiencing exactly one impact (Cases 1.1 and 1.2 in Fig. 4). In general, and as expected, the overturning-with-impact mode (Cases 1.1 and 1.2) is more critical, because it appears for lower excitation intensities. In the original (unretrofitted) system, energy is dissipated only through impacts, hence the overturning without impact mode is unaffected by the coefficient of restitution. On the other hand, the addition of viscous damping affects both modes of overturning. Further, unlike for the addition of strength (discussed in the Anchored Rocking Motion Section), both overturning envelopes shrink consistently with increased damping (Fig. 5).

The presented results are focused on the transient response of the damped rocking block to finite duration excitations. This is partly because the response of the damped rocking block to harmonic excitation has been thoroughly investigated by Hogan (1992) and Lenci and Rega (2006), among others. But more importantly, one main advantage of the rocking system is that constant frequency rocking resonance is impossible because the effective frequency changes with the rocking amplitude. Further, harmonic ground motions, which could cause rocking resonance, would have to have a precise time-varying frequency, and are thus extremely unlikely (DeJong 2009). As a result, the transient response to finite pulses typically governs the seismic response. It is possible that the rocking motion could build up, because of multiple impulses, but the addition of damping would suppress rocking between impulses, mitigating multiple impulse amplification. However, while quantifying this effect is beyond the scope of this work, it should be considered.

Damped Rocking Motion: Numerical Approach

Based on the above benefits of linear damping (previous section), this section aims to provide a means of predicting overturning

J. Eng. Mech. 2012.138:963-972.

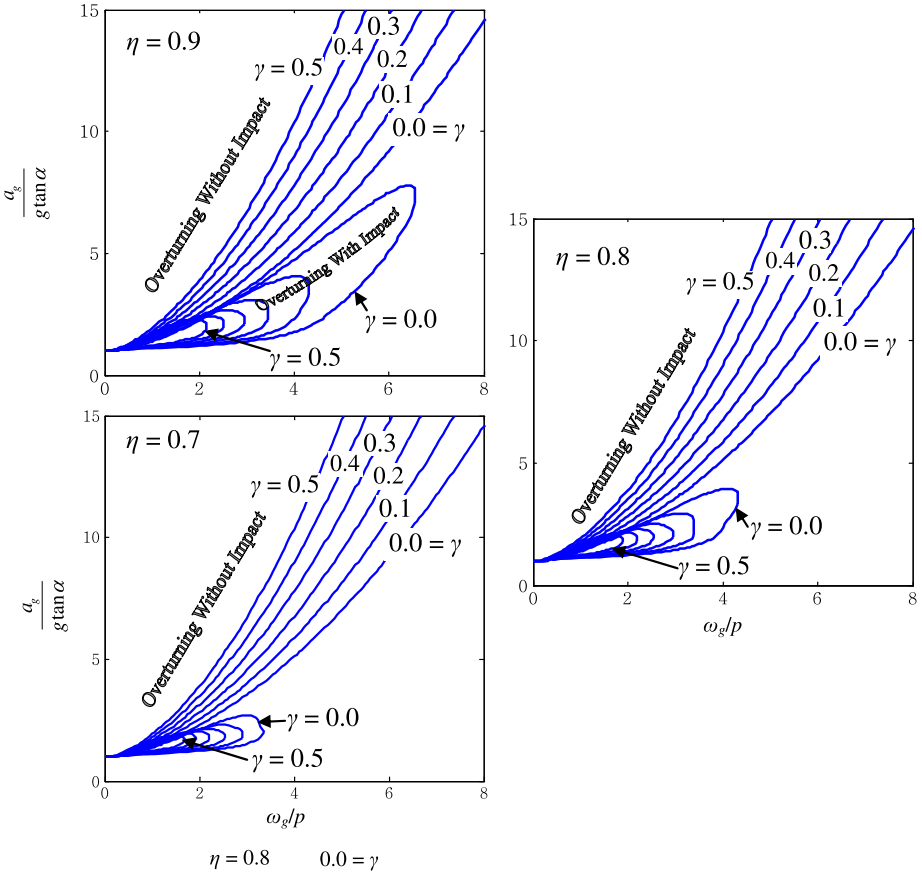

Fig. 5. Overturning envelopes of the damped rocking block under a sine pulse excitation for different coefficients of restitution η and different additional damping γ

envelopes for any damped rocking structure under any pulse-type ground motion. While the derivation is generally applicable, it will be specifically applied to investigate nonlinear viscous damping for both sine and cosine excitation pulses.

Bilateral Viscous Dampers

Consider the addition of (nonlinear) viscous dampers at the bottom corners of the rocking block (Fig. 3). The force P of a viscous nonlinear damper is given by

$$P = C|\dot{v}|^n \operatorname{sgn}(\dot{v}) \tag{14}$$

where $\dot{v}$ = extension velocity of the damper, C = damping constant, and n = damping exponent. Fig. 6 presents the force-velocity behavior of nonlinear viscous dampers. Moment equilibrium of the retrofitted rocking block gives

$$\ddot{\theta} = -p^2\left\{\sin[\alpha\operatorname{sgn}(\theta)-\theta] + \frac{\ddot{u}_g}{g}\cos[\alpha\operatorname{sgn}(\theta)-\theta]\right\} - p\gamma\left|\cos\frac{\theta}{2}\dot{\theta}\right|^n 2\cos\frac{\theta}{2}\operatorname{sgn}(\dot{\theta}) \tag{15}$$

where $\gamma = 3C\sin^2\alpha/(2mp)$ is again the dimensionless damping parameter. For linear viscous dampers, $n = 1$ and Eq. (15) simplifies to Eq. (5).

Unilateral Viscous Dampers

Recentering, or limiting residual displacements despite large displacement during seismic loading, is an advantage of the rocking motion. However, collapse must be prevented. Thus, to limit collapse while encouraging recentering, unilateral viscous dampers, which are activated only during uplift, are also considered. The behavior of unilateral viscous dampers can be described with the help of function $S_u(\theta,\dot{\theta})$

$$S_u(\theta,\dot{\theta}) = \frac{1}{2}[\operatorname{sgn}(\theta\cdot\dot{\theta})+1] = \begin{cases} 1 \text{ when uplifting} \\ 0 \text{ when restoring} \end{cases} \tag{16}$$

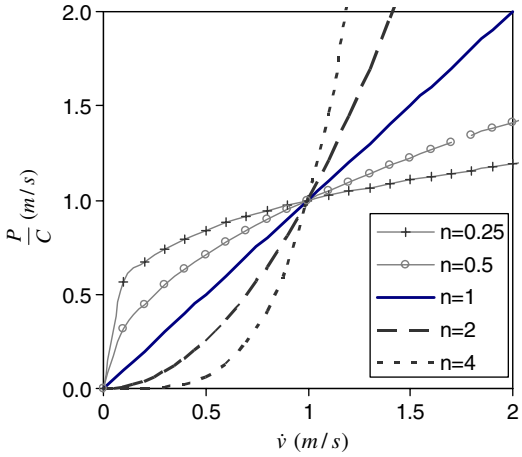

Fig. 6. Force (divided by damping constant) versus velocity behavior of nonlinear viscous dampers for different velocity exponents

J. Eng. Mech. 2012.138:963-972.

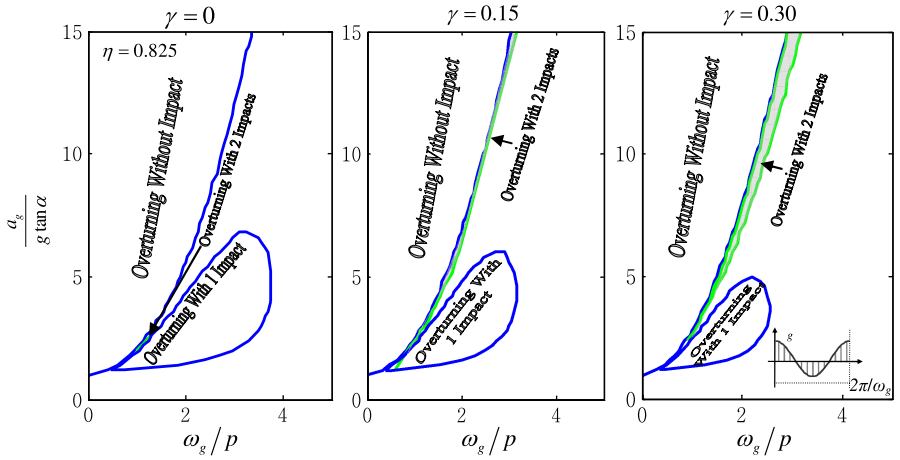

Fig. 7. Overturning envelopes, including the two impact overturning mode (shaded gray) for cosine pulse excitation and different levels of damping

From Eq. (15), the equation of motion for the linear unilateral viscous damper becomes

$$\ddot{\theta} = -p^2\left\{\sin[\alpha\,\mathrm{sgn}(\theta) - \theta] + \frac{\ddot{u}_g}{g}\cos[\alpha\,\mathrm{sgn}(\theta) - \theta]\right\} - p\gamma\left|\cos\frac{\theta}{2}\dot{\theta}\right|^n 2\cos\frac{\theta}{2}S_u(\theta,\dot{\theta})\mathrm{sgn}(\dot{\theta}) \tag{17}$$

Damped Rocking Response to Pulse-Type Excitations

The rocking response under single-cycle trigonometric pulse excitations is determined by numerically solving the nonlinear differential equations of motion [Eqs. (15) and (17)]. The numerical solutions are obtained through a state-space formulation using the differential equations solvers available in MATLAB. The pertinent results are presented using the same dimensionless terms of

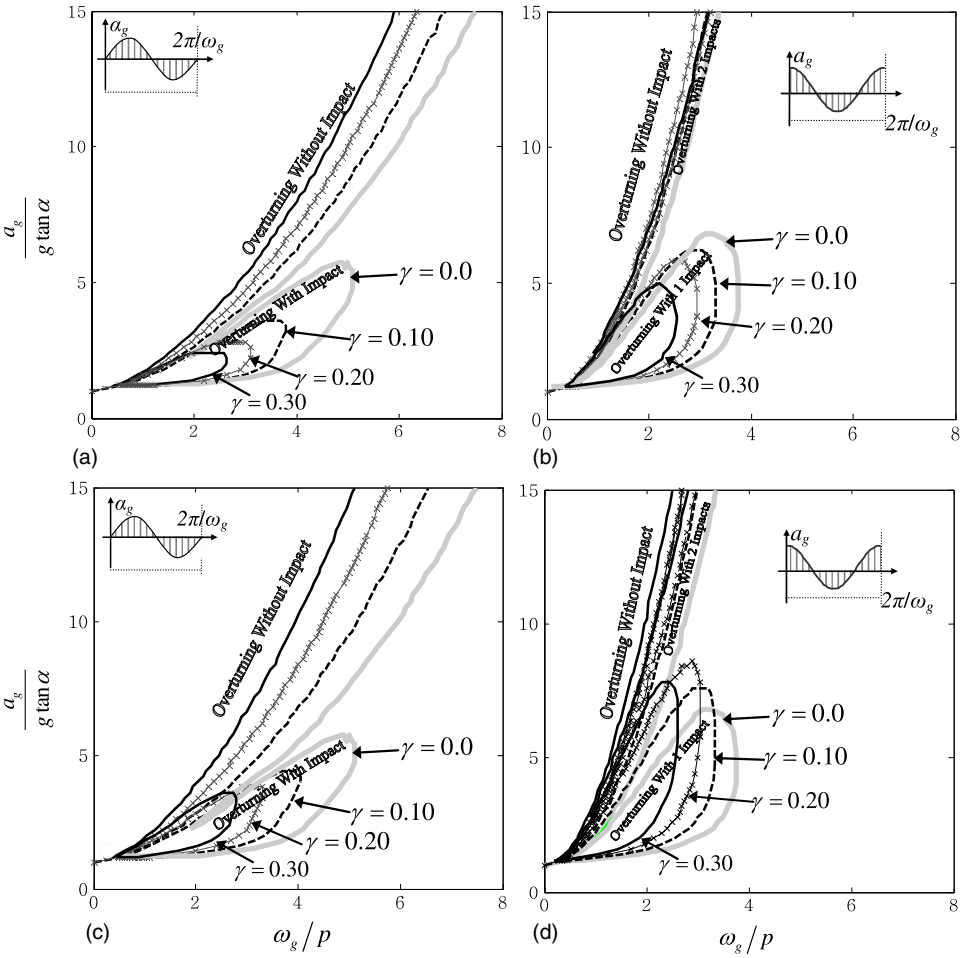

Fig. 8. (a)-(b) Overturning envelopes for the rocking block with bilateral linear viscous dampers; (c)-(d) unilateral linear viscous dampers; no damping (thick gray line)

J. Eng. Mech. 2012.138:963-972.

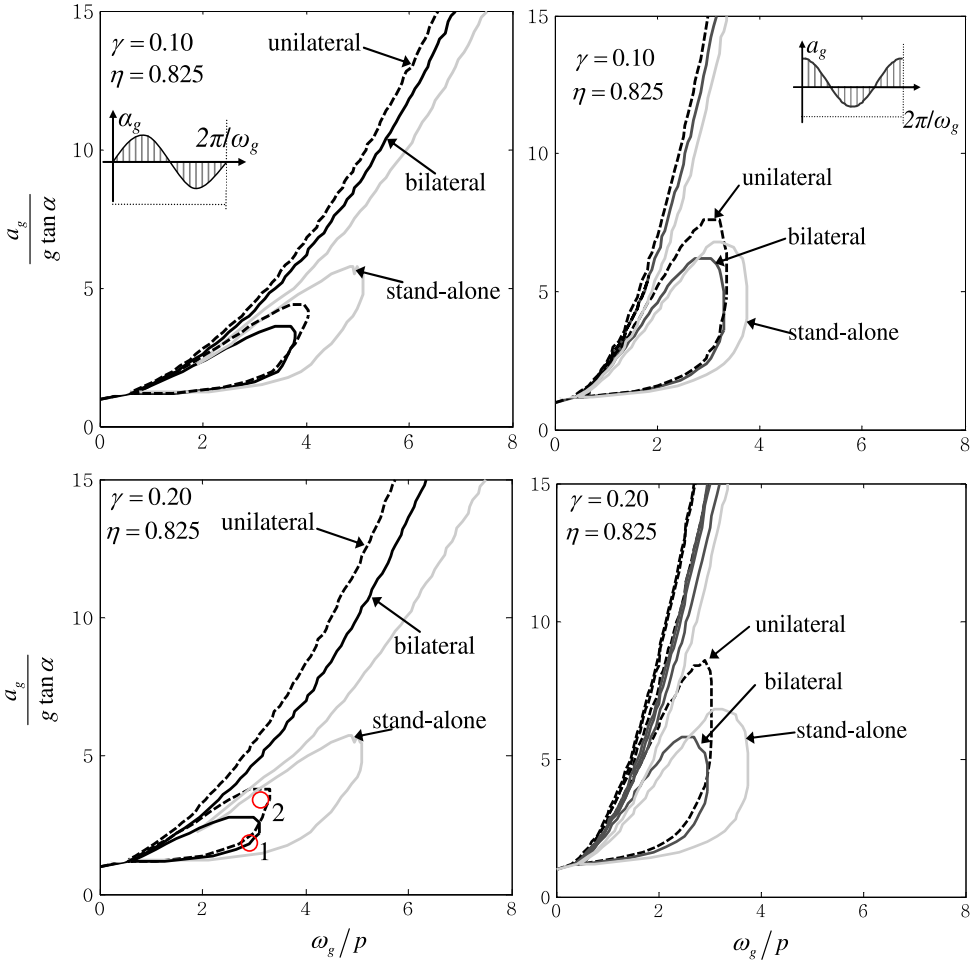

Fig. 9. Comparison of overturning envelopes for the rocking block retrofitted with bilateral and unilateral linear viscous dampers

Eq. (13) plus, in the case of nonlinear dampers, the velocity exponent n.

Linear Viscous Damping

As the previous sections indicate, a sine pulse excitation can cause overturning without impact or after exactly one impact. In addition, a two-impact overturning mode occurs for a cosine pulse, and more overturning modes arise for more complicated excitations (Hogan 1990; Hogan 1992; Plaut et al. 1996). The two-impact overturning mode for a cosine pulse is depicted in Fig. 7. It should be noted that the two-impact overturning region also exists for the undamped (stand-alone) rocking block, which has not been previously identified. Additional damping expands this overturning region (Fig. 7) for both bilateral and unilateral damping. The region associated with the two-impact overturning mode is relatively small and only slightly reduces the safe region between the no-impact and one-impact overturning modes. While this is of little consequence from a design perspective, it is interesting from a nonlinear dynamics perspective, and it further demonstrates the fickleness of the rocking response (Hogan 1990). In all subsequent figures, the lower limit of this two-impact overturning curve is plotted, while the no-impact overturning mode (which lies just above) is omitted for clarity.

Fig. 8 presents the overturning envelopes for bilateral damping, for equivalent unilateral damping (same γ parameter), and for the undamped (stand-alone) rocking block. Linear damping ($n = 1$) and a constant coefficient of restitution ($\eta = 0.825$) are assumed, and therefore the relationship between damping (γ) and the pulse characteristics, which cause collapse, can be directly portrayed. The overturning envelopes for sine pulses produced numerically from the fully nonlinear equations of motions are in good agreement with the pertinent semianalytical results of the Damped Rocking Motion: Semi-Analytical Approach Section.

The overturning envelopes shrink with additional damping for sine and cosine pulse excitations with both types of damping (though to a lesser extent with unilateral damping), although the safe region between the two modes of overturning is adversely shifted upward for the unilateral damping case (Fig. 9). Despite the favorable shrinking of the overturning region caused by damping, the beneficial upward shift of the low-frequency portion of the overturning envelope caused by the addition of strength (Fig. 2) is clearly not achieved by damping alone.

To clarify the relative effects of the two damping options, Fig. 9 directly compares the overturning envelopes for bilateral and unilateral damping. Both unilateral and bilateral dampers have a similar beneficial effect for overturning without impact. However, there is a brief change in velocity prior to overturning, during which the block tries to recover. Bilateral dampers limit this recovery, while unilateral dampers allow it, making them slightly more effective.

For overturning with impact, both damping options cause a similar beneficial shift in the minimum impulses, which cause overturning (the lower limit of the overturning area shifts up and left). However, bilateral dampers provide a larger decrease of the total overturning area through a larger downward shift in the

J. Eng. Mech. 2012.138:963-972.

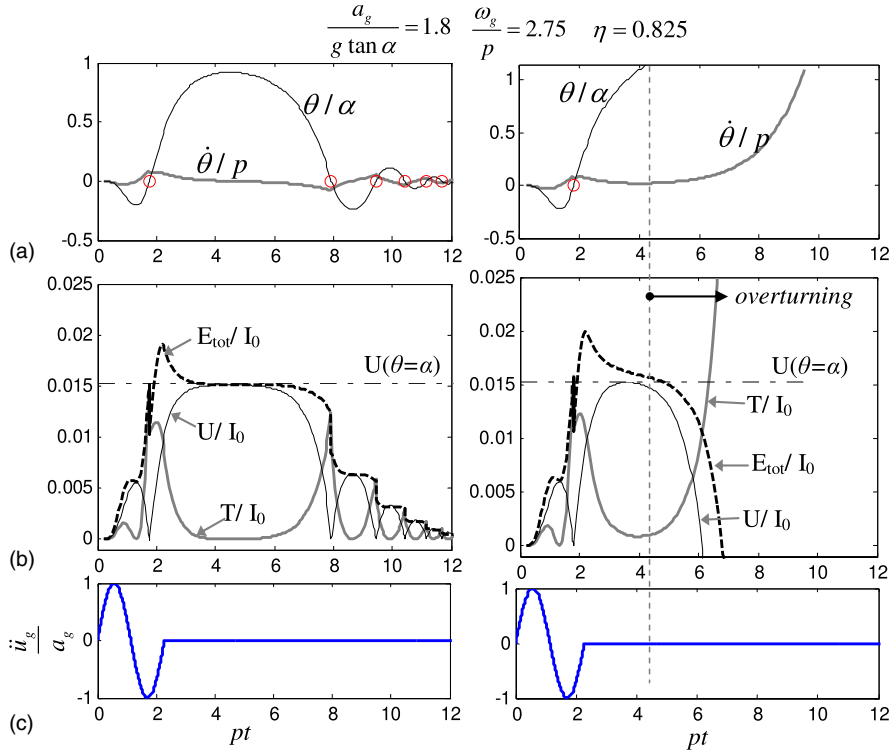

Fig. 10. (a) Comparison of the unilateral damping (left) and bilateral damping (right) rocking response and (b) system energies for identical rocking blocks excited with identical sine pulses (c) corresponding to Point 1 in Fig. 9

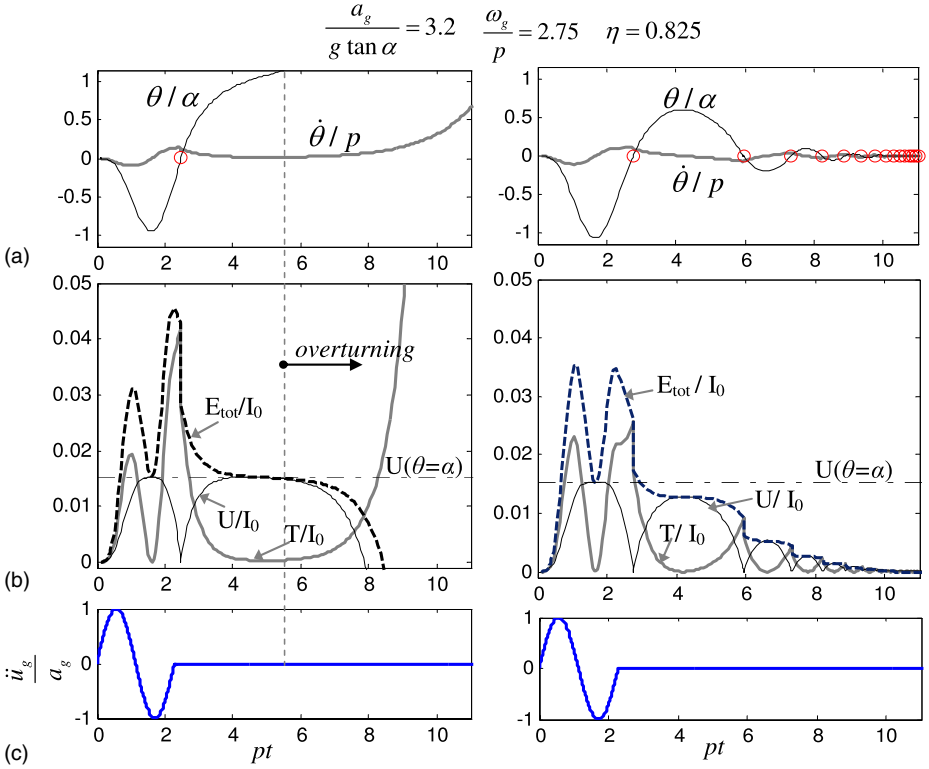

Fig. 11. (a) Comparison of the unilateral damping (left) and bilateral damping (right) rocking response and (b) system energies for identical rocking blocks excited with identical sine pulses (c) corresponding to Point 2 in Fig. 9

upper limit of the overturning region. While this may be beneficial, this intermediate safety area between the two overturning regions is a result of the highly nonlinear behavior of the rocking block and is very sensitive to the characteristics of the excitation (Hogan 1990; Plaut et al. 1996). As mentioned previously, it is not reliable from a design perspective and the lower limit is more important. Considering only the lower limit, both damping options have a remarkably similar benefit.

Figs. 10 and 11 further demonstrate the sensitivity of the rocking response by comparing specific energy time histories for which either bilateral damping or unilateral damping would be preferred. Figs. 10 and 11 present the rocking response corresponding to the Points 1 and 2, respectively, in the overturning diagram (Fig. 9), where T and U denote the kinetic and potential energy, E_{tot} is the total energy, and I_0 is the moment of inertia. In Fig. 10, bilateral damping results in overturning, while unilateral damping results in recovery. For the unilateral damping case, the total energy exceeds the minimum energy necessary for collapse, even after the acceleration pulse had ended, but the block recovers. In Fig. 11, both damping options nearly caused collapse without impact, and the bilateral damping case even exceeds the critical rotation ($|\theta/a| > 1$) before ultimately recovering. Furthermore, the maximum total system energy is more than twice the minimum energy necessary for collapse, but the block recovers because the maximum energy occurs when the potential energy (U) is minimal. Maximum total energy is clearly not a good indicator of collapse, because the energy input must synchronize with the rocking response to cause collapse.

Nonlinear Viscous Damping

While linear viscous dampers are effective in shrinking the overturning envelope, further benefit could be obtained by using nonlinear viscous dampers. Bilateral dampers performed slightly better than unilateral dampers, and therefore only bilateral nonlinear dampers will be considered. As n increases, the damping behavior resembles that of an impact absorber. As n decreases, the damping behavior tends toward frictional damping or a rigid-plastic behavior (see Fig. 6).

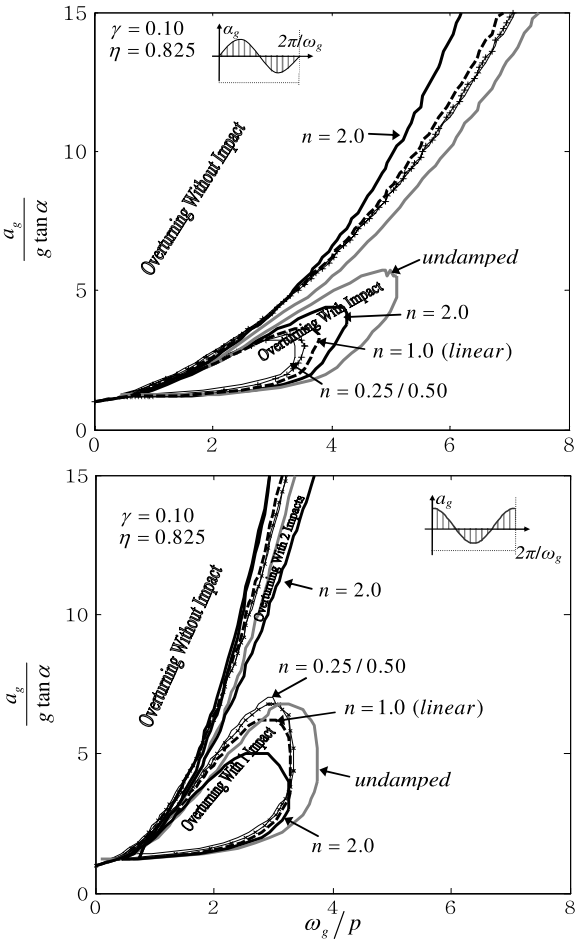

Fig. 12. Overturning envelopes for the rocking block with bilateral nonlinear viscous dampers and no damping (thick gray line)

Fig. 12 presents the single-pulse overturning envelopes for rocking blocks retrofitted with nonlinear dampers with various n coefficients. All types of nonlinear damping reduced the overturning envelope, but the effect of nonlinear damping compared with linear damping is markedly different for the two pulse types. For the sine pulse, the overturning envelope shrinks as n decreases, and expands as n increases. The inverse is true for the cosine pulse.

Therefore, a universal benefit for any pulse ground motion cannot be achieved by use of nonlinear damping. Instead, linear damping provides an average improvement for both types of ground motion.

Conclusions

The consequences of adding damping to rocking structures are investigated. Interestingly, while additional damping is already implemented in practice to retrofit rocking structures, there is a lack of theoretical research on the subject.

The overturning envelopes of a rocking block retrofitted with bilateral and unilateral (activated only during uplift) linear viscous dampers, show a substantial enhancement of the behavior. As a general rule, for a given damping level, the performance of the two types of damper is comparable. However, while the unilateral damper delays the first appearance of both the one-impact and no-impact overturning modes, the area of the one-impact overturning region is larger, compared with the pertinent bilateral damper results. In addition, nonlinear dampers have a moderate effect on the results, and provide contrasting shrinking or expansion of the overturning regions for the two pulse excitations investigated. Thus, linear damping seems an appropriate choice, for which the semianalytical approach provides a useful solution. Finally, in contrast to the alternative of anchoring the rocking system, the addition of damping does not lead to adverse effects, where the behavior of the retrofitted system may actually be worse than that of the stand-alone system.

Appendix. Analytical Solutions to Eq. 8

The constants A and B depend on the initial conditions of each response stage (Fig. 4) and the time instant the phase initiates. For zero initial conditions, $\theta(t=0) = \theta_0$, $\dot{\theta}(t=0) = \dot{\theta}_0$, they simplify to

$$A_0 = (\lambda - \mu)^{-1} \left\{ \frac{p^2 a_g}{\lg} [\mu \sin(\psi + \phi) - \omega_g \cos(\psi + \phi)] - \mu\alpha \right\}$$
$$B_0 = (\mu - \lambda)^{-1} \left\{ \frac{p^2 a_g}{\lg} [\lambda \sin(\psi + \phi) - \omega \cos(\psi + \phi)] - \lambda\alpha \right\} \tag{18}$$

After the end of the excitation and assuming no impact has taken place (Cases 1.2 and 2 of Fig. 4)

$$A_{ex0} = A_0 e^{\lambda T_{ex}} + (\lambda - \mu)^{-1} \frac{p^2 a_g}{gl} (\omega_g \cos\phi - \mu \sin\phi)$$
$$B_{ex0} = B_0 e^{\mu T_{ex}} + (\mu - \lambda)^{-1} \frac{p^2 a_g}{gl} (\omega_g \cos\phi - \lambda \sin\phi) \tag{19}$$

In the event of an impact after the end of the excitation (Case 1.2 of Fig. 4), the time instant impact occurs t_{i2} is determined by solving

J. Eng. Mech. 2012.138:963-972.

$$-\alpha + A_{ex0}e^{\lambda(t_{i2}-T_{ex})} + B_{ex0}e^{\mu(t_{i2}-T_{ex})} = 0 \tag{20}$$

where the pertinent overturning condition is

$$B_{i2} = (\mu-\lambda)^{-1}\left[\eta(\lambda A_{ex0}e^{\lambda(t_{i2}-T_{ex})} + \mu B_{ex0}e^{\mu(t_{i2}-T_{ex})}) + \lambda\alpha\right] = 0 \tag{21}$$

On the other hand, if an impact occurs before the end of the excitation (Case 1.1 of Fig. 4)

$$\begin{aligned}
\dot{\theta}(t_{i1}) &= \dot{\theta}_{i1} = \lambda A_0 e^{\lambda t_{i1}} + \mu B_0 e^{\mu t_{i1}} + \frac{p^2 a_g \omega_g}{gl}\cos(\omega_g t_{i1} + \psi + \phi) \\
A_{i1} &= (\lambda-\mu)^{-1}\Big\{\eta\dot{\theta}_{i1} + \mu\alpha + \frac{p^2 a_g}{gl}[\mu\sin(\omega_g t_{i1} + \psi + \phi) \\
&\quad - \omega\cos(\omega_g t_{i1} + \psi + \phi)]\Big\} \\
B_{i1} &= (\mu-\lambda)^{-1}\Big\{\eta\dot{\theta}_{i1} + \lambda\alpha + \frac{p^2 a_g}{gl}[\lambda\sin(\omega_g t_{i1} + \psi + \phi) \\
&\quad - \omega\cos(\omega_g t_{i1} + \psi + \phi)]\Big\}
\end{aligned} \tag{22}$$

where the time instant of impact t_{i1} (Case 1.1 of Fig. 4) is determined by solving

$$-\alpha + A_0 e^{\lambda t_{i1}} + B_0 e^{\mu t_{i1}} + \frac{p^2}{l}\frac{a_g}{g}\sin(\omega_g t_{i1} + \psi + \phi) = 0 \tag{23}$$

The rotation and the angular velocity of the block at the end of the excitation become

$$\begin{aligned}
\theta_{ex} &= \theta(T_{ex} - t_{i1}) = \alpha + A_{i1}e^{\lambda(T_{ex}-t_{i1})} + B_{i1}e^{\mu(T_{ex}-t_{i1})} + \frac{p^2 a_g}{gl}\sin\phi \\
\dot{\theta}_{ex} &= \dot{\theta}(T_{ex} - t_{i1}) = \lambda A_{i1}e^{\lambda(T_{ex}-t_{i1})} + \mu B_{i1}e^{\mu(T_{ex}-t_{i1})} + \frac{p^2 a_g \omega_g}{gl}\cos\phi
\end{aligned} \tag{24}$$

The overturning condition accordingly becomes

$$B_{ex1} = (\mu-\lambda)^{-1}(\dot{\theta}_{ex} + \lambda\alpha - \lambda\theta_{ex}) = 0 \tag{25}$$

Acknowledgments

Financial support for this research was provided by the Engineering and Physical Sciences Research Council of the United Kingdom under Grant no. EP/H032657/1.

References

Ajrab, J. J., Pekcan, G., and Mander, J. B. (2004). "Rocking wall—frame structures with supplemental tendon systems." *J. Struct. Eng.*, 130(6), 895–904.

Augusti, G., and Sinopoli, A. (1992). "Modelling the dynamics of large block structures." *Meccanica*, 27(3), 195–211.

Caliò, I., and Marletta, M. (2003). "Passive control of the seismic rocking response of art objects." *Eng. Struct.*, 25(8), 1009–1018.

Chen, Y., Liao, W., Lee, C., and Wang, Y. (2006). "Seismic isolation of viaduct piers by means of a rocking mechanism." *Earthquake Eng. Struct. Dyn.*, 35(6), 713–736.

Cheng, C. (2007). "Energy dissipation in rocking bridge piers under free vibration tests." *Earthquake Eng. Struct. Dyn.*, 36(4), 503–518.

Contento, A., and Di Egidio, A. (2009). "Investigations into the benefits of base isolation for non-symmetric rigid blocks." *Earthquake Eng. Struct. Dyn.*, 38(7), 849–866.

DeJong, M. J. (2009). "Seismic assessment strategies for masonry structures." Ph.D. thesis, Massachusetts Institute of Technology, Cambridge, MA.

DeJong, M. J., De Lorenzis, L., Adams, S., and Ochsendorf, J. A. (2008). "Rocking stability of masonry arches in seismic regions." *Earthquake Spectra*, 24(4), 847–865.

Di Egidio, A., and Contento, A. (2009). "Base isolation of slide-rocking non-symmetric rigid blocks under impulsive and seismic excitations." *Eng. Struct.*, 31(11), 2723–2734.

ElGawady, M. A., and Sha'lan, A. (2011). "Seismic behavior of self-centering precast segmental bridge bents." *J. Bridge Eng.*, 16(3), 328–339.

Hogan, S. J. (1990). "The many steady state responses of a rigid block under harmonic forcing." *Earthquake Eng. Struct. Dyn.*, 19(7), 1057–1071.

Hogan, S. J. (1992). "The effect of damping on rigid block motion under harmonic forcing." *Proc. R. Soc. A*, 437(1899), 97–108.

Hung, H., Liu, K., Ho, T., and Chang, K. (2011). "An experimental study on the rocking response of bridge piers with spread footing foundations." *Earthquake Eng. Struct. Dyn.*, 40(7), 749–769.

Lenci, S., and Rega, G. (2006). "A dynamical systems approach to the overturning of rocking blocks." *Chaos Solitons Fractals*, 28(2), 527–542.

Makris, N., and Roussos, Y. (1998). "Rocking response and overturning of equipment under horizontal pulse-type motions." *PEER-1998/05*, *Pacific Earthquake Engineering Research Center*, Univ. of California, Berkeley, CA.

Makris, N., and Zhang, J. (2001). "Rocking response of anchored blocks under pulse-type motions." *J. Eng. Mech.*, 127(5), 484–494.

Marriott, D., Pampanin, S., and Palermo, A. (2009). "Quasi-static and pseudo-dynamic testing of unbonded post-tensioned rocking bridge piers with external replaceable dissipaters." *Earthquake Eng. Struct. Dyn.*, 38(3), 331–354.

Pampanin, S. (2006). "Controversial aspects in seismic assessment and retrofit of structures in modern times: Understanding and implementing lessons from ancient heritage." *Bull. New Zeal. Soc. Earthquake Eng.*, 39(2), 120–133.

Plaut, R., Fielder, W., and Virgin, L. (1996). "Fractal behavior of an asymmetric rigid block overturning due to harmonic motion of a tilted foundation." *Chaos Solitons Fractals*, 7(2), 177–196.

Pollino, M., and Bruneau, M. (2007). "Seismic retrofit of bridge steel truss piers using a controlled rocking approach." *J. Bridge Eng.*, 12(5), 600–611.

Rai, D. C., and Goel, S. C. (2007). "Seismic strengthening of rocking-critical masonry piers." *J. Struct. Eng.*, 133(10), 1445–1453.

Restrepo, J. I., and Rahman, A. (2007). "Seismic performance of self-centering structural walls incorporating energy dissipators." *J. Struct. Eng.*, 133(11), 1560–1571.

Roh, H., and Reinhorn, A. M. (2010). "Modeling and seismic response of structures with concrete rocking columns and viscous dampers." *Eng. Struct.*, 32(8), 2096–2107.

Ugalde, J. A., Kutter, B. L., and Jeremic, B. (2010). "Rocking response of bridges on shallow foundations." *PEER Report 2010/101*. Pacific Earthquake Engineering Research Center College of Engineering, Univ. of California, Berkeley, CA.

Vassiliou, M. F., and Makris, N. (2012). "Analysis of the rocking response of rigid blocks standing free on a seismically isolated base." *Earthquake Eng. Struct. Dyn.*, 41(2), 177–196.

Zhang, J., and Makris, N. (2001). "Rocking response of free-standing blocks under cycloidal pulses." *J. Eng. Mech.*, 127(5), 473–484.